APL Materials

RESEARCH ARTICLE | MAY 11 2026

Enhancement of corrosion resistance, hardness, and biosafety for martensitic stainless steel via laser thermal processing

Y. Tsutsumi ✉ ; M. Shimabukuro ; T. Manaka ; M. Goto ; M. Kaodowaki ; T. Hashimoto ; M. Kawashita ; T. Ishimoto ; H. Katayama

APL Mater. 14, 051105 (2026)
https://doi.org/10.1063/5.0334196

Enhancement of corrosion resistance, hardness, and biosafety for martensitic stainless steel via laser thermal processing

Cite as: APL Mater. 14, 051105 (2026); doi: 10.1063/5.0334196
Submitted: 17 March 2026 • Accepted: 22 April 2026 •
Published Online: 11 May 2026

Y. Tsutsumi,[1,2,a] M. Shimabukuro,[3] T. Manaka,[4] M. Goto,[5] M. Kaodowaki,[1] T. Hashimoto,[1] M. Kawashita,[3] T. Ishimoto,[6] and H. Katayama[1]

AFFILIATIONS

[1] Research Center for Structural Materials, National Institute for Materials Science, Tsukuba, Japan
[2] Department of Materials Science and Engineering, School of Materials and Chemical Technology, Institute of Science Tokyo, Tokyo, Japan
[3] Laboratory for Biomaterials and Bioengineering, Institute of Integrated Research, Institute of Science Tokyo, Tokyo, Japan
[4] School of Sustainable Design, University of Toyama, Toyama, Japan
[5] Fuji Koushuha Industry Co. Ltd., Sakai, Japan
[6] Titanium Research Center, University of Toyama, Toyama, Japan

[a] **Author to whom correspondence should be addressed:** TSUTSUMI.Yusuke@nims.go.jp

ABSTRACT

A laser thermal processing technique was used to efficiently improve the corrosion resistance of 420J2 martensitic stainless steel. The top layer of the steel plate was melted and immediately solidified by properly controlled laser irradiation. After the processing, the surfaces of the specimens were oxidized. The roughened oxidized layer that formed on the as-processed specimen was removed by grinding to expose the remelted layer. Potentiodynamic anodic polarization measurements confirmed that the remelted layer showed much better corrosion resistance. Furthermore, the hardness of the remelted layer increased to 700 HV. To evaluate the initial cell activity of the processed steel, osteoblast-like cell line (MC3T3-E1) was used. The initial proliferation of the cells was significantly improved on the laser-processed stainless steel. Therefore, laser thermal processing is a useful tool for developing novel materials with a combination of hardness, corrosion resistance, and cytocompatibility.

I. INTRODUCTION

Stainless steel is a major corrosion-resistant material used in various industries. Stainless steels exhibit different crystallographic structures depending on their composition and heat treatment. Therefore, they are classified into several types: ferritic, austenitic, duplex, precipitation hardening, and martensitic. Among these, martensitic stainless steels are distinguished by their ability to undergo hardening through a simple heat treatment (quenching).[1] However, for this hardening property, the use of carbon, which reduces corrosion resistance, is inevitable. In addition, owing to the limited Ni content of martensitic stainless steels, they have the lowest corrosion resistance among all types of stainless steels. Therefore, the greatest advantage of martensitic stainless steels is their hardness, which is acquired by sacrificing corrosion resistance.[2,3] Precipitation-hardening stainless steels can also be hardened by a specific heat treatment (aging) and exhibit a relatively higher corrosion resistance than martensitic stainless steels; however, their hardness range is slightly lower than that of martensitic stainless steels. The corrosion resistance of precipitation-hardening stainless steel is inferior to that of austenitic stainless steel. Furthermore, metal ions are released as a result of the corrosion reaction, while copper and nickel that are harmful to living organisms are contained in precipitation-hardening stainless steel, making it unsuitable for medical applications. Therefore, austenitic stainless steel (type 316L), exhibiting sufficient corrosion resistance, is employed for medical devices implanted in the living body for long-term usage. On the other hand, martensitic stainless steels are primarily used

in specific instruments, such as surgical blades, cutting edges, and injection needles. This is because their contact with living tissue is brief, and any metal ion release resulting from corrosion reactions is minimal and considered insignificant.

Hence, achieving both high hardness and corrosion resistance in stainless steels is generally difficult.[4]

In recent years, studies on the corrosion resistance of stainless steels fabricated by additive manufacturing (AM) have attracted considerable attention.[5–9] The authors have investigated the corrosion resistance of metallic materials using the AM process. Stainless steels manufactured by using the laser powder-bed fusion (LPBF) process show extremely high corrosion resistance compared to that of commercially available steel.[10,11] This significant enhancement in the corrosion resistance of the LPBF steel was attributed to the extremely fast cooling rate during solidification. Corrosion-inducing inclusions, such as manganese sulfide (MnS),[12–17] do not allow sufficient time for nucleation and growth during solidification. This means that the surface of the stainless steel produced by LPBF is virtually free of MnS, which is found in commercial materials. Consequently, the surface of the stainless steel obtained via the LPBF process shows minimal exposure to the MnS inclusions that are always found on general steels obtained via a normal manufacturing process.

Thus, LPBF processes realize the specific microstructure due to the ultra-rapid cooling thermal history, resulting in the suppression of corrosion-inducing inclusions that degrade corrosion resistance in stainless steels. On the other hand, manufacturing products via AM processes such as LPBF have limitations in production size, processing time, and cost due to the requirement of metal powders as raw materials. While AM is reasonably compatible with both small-sized and high-value-added products such as medical devices, in the case of large-sized or ready-made products, achieving high corrosion resistance through AM is not feasible.

Therefore, in this study, we investigated a laser surface remelting process originally developed as a laser surface quenching technique for high carbon containing and martensitic stainless steels. The laser power was adjusted to ensure the formation of melting on limited surface area and the beam was scanned at a constant rate. Consequently, the top layer of the laser-scanned area on the steel was covered by a thin remelted layer, which had a special thermal history of a super-rapid cooling rate, similar to the LPBF process. This specific metal structure formed on the steel surface through this laser thermal processing is expected to provide excellent corrosion resistance by suppressing the formation of corrosion-inducing inclusions, as in the case of LPBF.

In this study, a common martensitic stainless steel grade, type 420J2, was subjected to laser thermal processing with controlled power, enabling localized melting, followed by rapid solidification. The corrosion resistances and hardnesses of the laser-processed specimens were also evaluated. In addition, the initial proliferation of an osteoblast-like cell line (MC3T3-E1) was evaluated to determine the cytocompatibility and biosafety of the specimens.

II. MATERIALS AND METHODS

A. Specimen preparation

A martensitic-type 420J2 stainless steel plate ($40 \times 80 \times 5$ mm^3) was used in this study. The specimens were solution treated and annealed in advance. Before the laser process, the surfaces of the specimens were mechanically ground using a No. 800 abrasive SiC paper. The specimens were then subjected to laser thermal processing using a high-power semiconductor laser oscillator (LDF5000-100, Laserline GmbH, Germany), according to the following procedure: The specimens were laser-irradiated at a beam width of 10 mm and a scanning rate of 1000 mm min^{-1} under open-air conditions using a laser power of about 3250 W. After processing, the surfaces of the specimens were ground again to remove the thermally oxidized layer and to flatten the slightly concavo-convex laser tracks for subsequent corrosion resistance and cell viability evaluations.

Surface observations using a scanning electron microscope (TM4000Plus, Hitachi High-Tech Corp., Japan) were performed to characterize the exposed inclusions on the specimen surface before and after the laser processing.

B. Corrosion resistance evaluation

The corrosion resistance of stainless steel specimens with and without subsequent thermal treatment was evaluated by potentiodynamic anodic polarization measurements (linear sweep voltammetry), as described in our previous study.[10,11,18,19] The measurements were performed using a potentiostat (HABF-501G, Hokuto Denko, Japan) connected to a function generator (HB-111, Hokuto Denko, Japan) via an analog cable. A standard silver–silver chloride electrode (Ag/AgCl) with a saturated KCl internal solution and a platinum electrode were used as the reference and counter electrodes, respectively.

Except for the area to be measured, the specimen surface was coated with an insulating resin paint. Therefore, only the area of the laser-irradiated track was in contact with the test solution. For comparison, a specimen without laser irradiation (unprocessed) was coated in the same manner and its corrosion resistance was evaluated. The exposed area in contact with the electrolyte was 0.7 cm^2. After contacting the chloride-containing corrosion testing solution (0.1 mol l^{-1} Na_2SO_4 and 0.585 mol l^{-1} NaCl, aerated at 25 °C), open circuit condition was maintained for 10 min. A gradient anodic potential was then applied at a constant sweep rate of 1 mV s^{-1} from the initial negative potential of 50 mV to the final value of the open-circuit potential (OCP). The measurement was stopped when the breakdown of the passive film occurred and the current density reached 1 mA cm^{-2}.

C. Cell proliferation evaluation

MC3T3-E1 cells were used to evaluate initial cytocompatibility. Cells were cultured in a specific medium, which was a mixture of alpha-modified Eagle's minimum essential medium (α-MEM) with 10% fetal bovine serum and 1% antibiotics. All the specimens were sterilized by immersion in 70% ethanol. Because the laser-irradiated area was limited to a straight line 10 mm in width, glass cylinders (cloning rings) with an inner diameter of 7 mm were placed on the irradiated area, and the interfaces between the cylinders and the specimen surface were sealed using non-toxic grease, as shown in Fig. 1. The cells were then seeded inside glass cylinders fixed on the specimens at an initial density of 1000 cells/cylinder (2598 cells/cm^2). The number of living cells 24 and 48 h after seeding was measured using a cell counting kit (CCK-8; Dojindo Laboratories, Kumamoto, Japan). Absorbance at 450 nm was measured using a

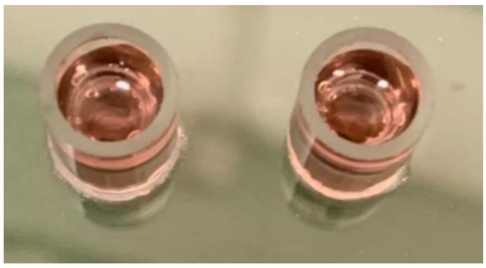

FIG. 1. Setup for cell culture on stainless-steel plate specimen surfaces. Glass cylinders with an inner diameter of 7 mm were loosely bonded to the steel surface with non-toxic grease to prevent leakage of the culture medium.

microplate reader. As a control, a pure titanium (Ti) plate and a culture dish (tissue culture polystyrene, TCPS) were prepared and tested under the same conditions as the stainless steel specimens. Cell number data were obtained from six independent areas for each specimen, and the mean and standard deviation were calculated. ANOVA and Student–Newman–Keuls multiple comparison tests were used for statistical analysis in this study.

III. RESULTS AND DISCUSSION

A. Phase transformation and hardness change by laser irradiation

The appearance and cross-sectional images of the specimens after the laser thermal processing are shown in Fig. 2. After laser irradiation, the surface of the specimen changed to a slightly brownish-white surface owing to atmospheric oxidation by residual heat, in addition to changes in the surface roughness because of the remelting and solidification history. However, this change in appearance was nearly consistent with a laser width of 10 mm, indicating that only the irradiated area was intensively heated and the melting zone was controlled to be minimized only at the targeted area.

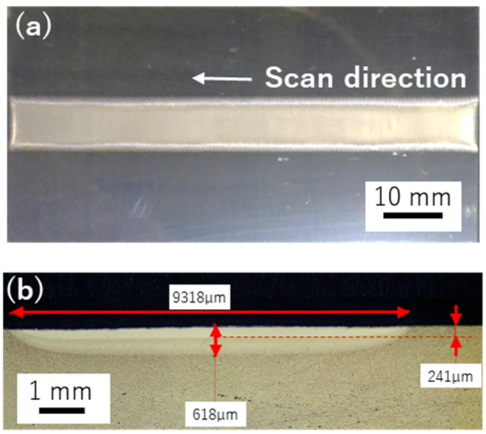

FIG. 2. (a) Photograph of the surface of a stainless steel specimen sheet after the laser thermal processing, and (b) photograph of the cross section of a specimen near the laser irradiation area.

The cross-sectional image [Fig. 2(b)] shows that multiple new layers had formed under the steel surface, where the laser was irradiated under appropriate power conditions, in a shallow area less than 1 mm in depth. In the case of the laser-quenching process (lower than 1000 W in machine power), which involved only heating without melting, the resulting structure exhibited only one new layer. This suggests that these layers are actually remelted, followed by super-rapid solidification (upper layer: liquid-to-solid phase) and phase transformation (lower layer: solid-to-solid phase).

Based on these results, to conduct further experiments, the specimen was ground to completely remove the rough oxidized outermost layer, followed by polishing to a surface finish of No. 800. The thickness reduction in this additional grind and polishing process was ~50 μm, confirming that both corrosion resistance and cell viability tests are performed on the surface of the remelted layer.

The hardness of the remelted layer was 700 HV, which is much higher than that of the unprocessed specimen (175 HV). As 700 HV (Vickers hardness) corresponds to 60–61 HRC (Rockwell C hardness), the remelting layer was confirmed to have reached the highest level of hardness in this steel grade (Type 420J2).

B. Corrosion resistance

Figure 3 shows the polarization curves of the unprocessed specimen in the chloride-containing testing solution. To confirm the reproducibility, the test was repeated five times under the same conditions. The unprocessed specimen exhibited unstable current density fluctuations immediately after the potential sweep started and 10 min after the open-circuit condition. The temporally rapid rise in current and subsequent rapid drop in current to the baseline represent the breakdown and repassivation of the passive film, respectively. This indicates the repetitive occurrence of typical metastable pitting corrosion. After reaching a certain potential, the current kept increasing rapidly without decreasing. This indicates that a stable (growing) pitting corrosion occurred. In this study, the

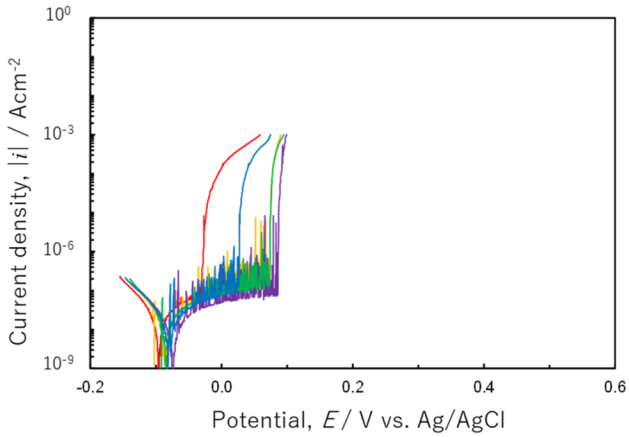

FIG. 3. Polarization curves of the unprocessed stainless steel in NaCl and Na_2SO_4 mixed testing solution. The regions where the line segments appear to be broadened and brushed out are the result of the repetitive current fluctuation over a short span, indicating the high frequency of metastable pitting corrosion occurrence.

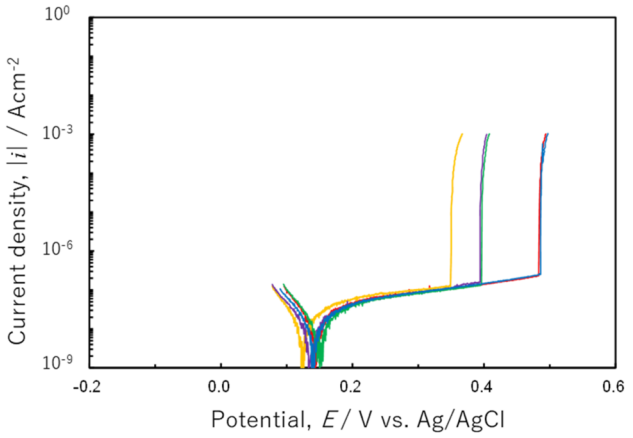

FIG. 4. Polarization curves of the laser thermal processed stainless steel specimens in Na_2SO_4 mixed testing solution.

pitting potential (E_{pit}) is defined as the potential at which the current density reaches the threshold of 100 μA cm^{-2}. For unprocessed specimen, E_{pit} ranged 56 ± 39 mV vs Ag/AgCl (mean ± standard deviation, respectively).

Figure 4 shows the polarization curves of the laser-processed specimens. The shapes of the polarization curves of the laser-processed specimens apparently differed from those of the unprocessed specimens, and the current density was stable over a wide range of applied potentials, indicating passive regions. The E_{pit} value of the laser processed specimens ranged 424 ± 60 mV vs Ag/AgCl and it is significantly larger than that of the unprocessed specimen. These results indicate that the corrosion resistance of 420J2 martensitic stainless steel can be significantly improved by laser thermal processing.

Notably, the polarization curves in Fig. 4 show nearly no signs of metastable pitting. This suggests that the remelting layer formed by laser irradiation contained almost no corrosion-inducing inclusions that could act as initiation sites for stable or metastable pitting corrosion. The specific polarization curve without metastable pitting in this study is similar to the results for stainless steels produced by the LPBF process in our previous study.[10,11]

C. Characterization of inclusions

To investigate the distribution of inclusions, SEM observation was performed. Figure 5(a) shows a microscopic image of an as-received stainless steel specimen with mirror-finishing polish. Numerous isotropic particles of inclusions were distributed over the steel matrix. Furthermore, relatively larger particles elongated in the working process direction were also observed. EDS mapping analysis results at the same location are shown in Fig. 5(b). The equiaxed fine particles were identified as Cr-based oxide inclusions, characterized by high Cr and O and low Fe concentrations, indicating preferential oxidation of Cr. The elongated large particles exhibited high Mn and S concentrations, confirming the presence of corrosion-inducing MnS inclusions.

Figure 6 shows the SEM/EDS results of laser-processed specimen polished in the same manner. Spherical particles of

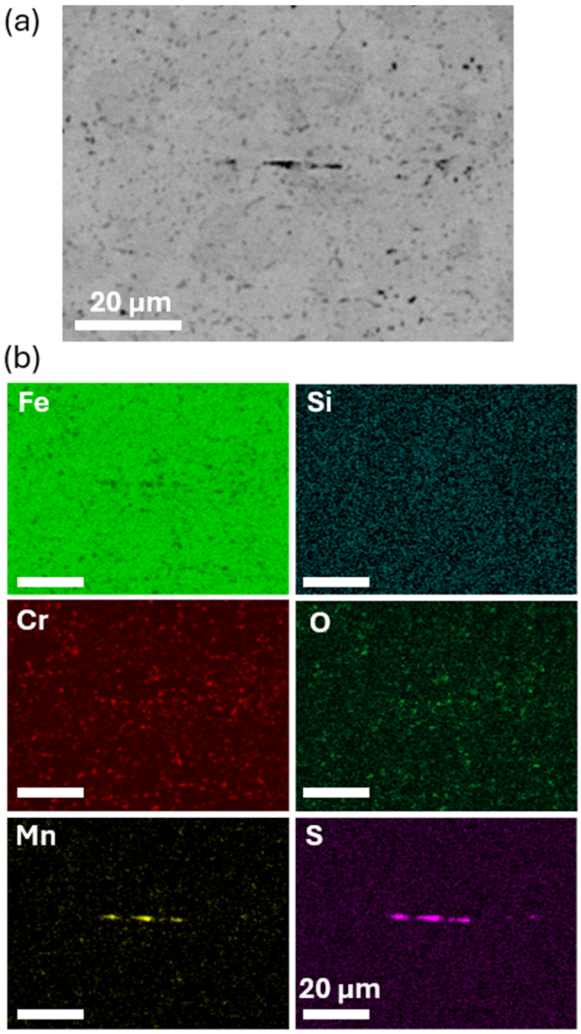

FIG. 5. Results of SEM/EDS analysis of the as-received stainless steel specimen. (a) Backscattered electron image and (b) EDS mapping images.

submicrometer size were observed on this specimen. From EDS results, they were found to be mainly Si oxide-based inclusions. On the other hand, MnS was not observed on the laser-processed specimen although the entire surface was carefully examined. It is difficult to definitively prove through microscopic observation that corrosion-inducing MnS inclusions had been completely removed by laser processing. However, the occurrence of localized corrosion on stainless steels caused by MnS inclusions is significantly influenced by their size and morphology. Therefore, the reduction in both the number and size of MnS inclusion particles is considered to have contributed to the significant improvement in localized corrosion resistance, as shown in Figs. 3 and 4.

The principle of this technique is improving the inherent corrosion resistance of the stainless steel substrate itself rather than coating its surface. Therefore, excellent corrosion resistance will be retained even during long-term applications.

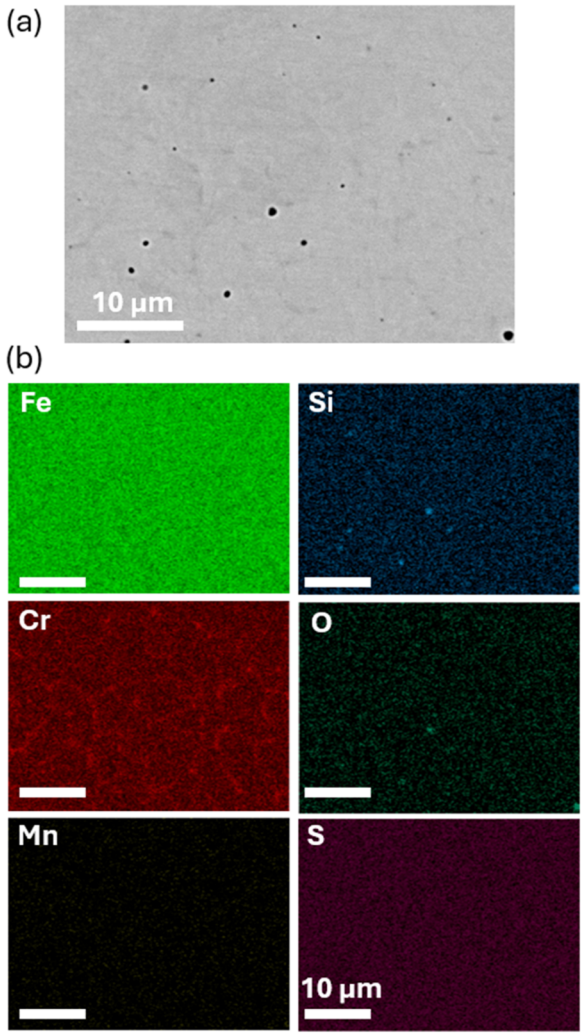

FIG. 6. Results of SEM/EDS analysis of the laser thermal processed stainless steel specimen. (a) Backscattered electron image and (b) EDS mapping images.

D. Cell proliferation

The results of the cell proliferation tests are shown in Fig. 7. The test was also performed on TCPS dishes and pure Ti plates as references, in addition to stainless steel specimens with and without laser thermal processing. All the specimens exhibited cell growth for up to 48 h after seeding. Therefore, although the degree of cell proliferation differed, none of the specimens exhibited cytotoxic properties. However, the unprocessed stainless steel specimen showed a significantly lower cell density than the laser-processed specimen 24 h after seeding. After 48 h from seeding, the cell density of the unprocessed specimen increased considerably; however, the order remained unchanged, resulting in a significantly lower cell density than that of the laser-processed and pure Ti specimens. This indicates that in the initial stage of the test, the adhesion and proliferation of cells were inhibited owing to the release of metal ions caused by the temporal corrosion reaction occurring on the unprocessed steel surface. On the other hand, there was no significant difference in cell density between the laser-processed stainless steel and Ti specimens 24 and 48 h after seeding. Therefore, it was demonstrated that laser thermal processing effectively inhibits the corrosion reaction and improves the cytocompatibility of martensitic stainless steel to comparable with Ti.

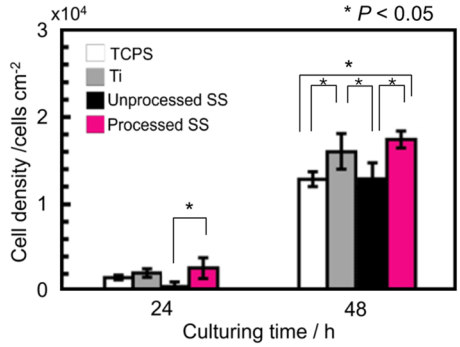

FIG. 7. Results of osteoblast-like cell line (MC3T3-E1) tests after 24 and 48 h from seeding. Cells were seeded at an initial density of 2598 cells/cm^2, with the results of 24 and 48 h mainly representing the initial adhesion and proliferation activity, respectively.

E. Advantages and limitations of laser thermal processing treatment

This study demonstrated that laser thermal processing simultaneously achieves high corrosion resistance and hardness for martensitic stainless steel. It was also demonstrated that the surface of martensitic stainless steel could be improved to exhibit equivalent cytocompatibility with Ti without affecting the initial cell activities. However, limitations in this study should be referred to the practical application of this technique. To directly associate the results of the cell proliferation and corrosion resistance measurements, it is necessary to measure the amount of metal ions released into the cell culture medium. It has been reported that surgical-grade stainless steels are biosafe and generally exhibit minimal toxicity.[20] On the other hand, it has also been reported that martensitic stainless steels with relatively lower corrosion resistance exhibit cytotoxicity.[21] Even supermartensitic stainless steel (low-carbon and high-molybdenum) exhibits a certain degree of metal ion release resulting in cytotoxicity.[22] Since this study employed a typical high-carbon martensitic stainless steel (420J2), a certain degree of metal ion release had occurred on the unprocessed specimen during the initial stage of cell culturing. In contrast, it can be considered that this ion release was suppressed on the laser processed specimens.

As shown in Fig. 2(b), laser irradiation causing remelting resulted in the formation of two new layers. However, the corrosion resistance of the lower layer, which appears to have transformed into the martensitic phase, and the effects of differences in laser processing conditions should be clarified. Our latest research has also confirmed that, under conditions of excessive laser power, residual stresses cause cracks on the outermost surface layer, resulting in diminished corrosion resistance. To achieve the best performance, it is necessary to optimize the laser processing conditions according to

the specific grade of stainless steels. Further investigation is necessary to understand the variation in corrosion resistance in the depth direction.

We would like to continue to investigate the potential of laser thermal processing, including the evaluation of the effects of tempering heat treatment, to relax the super-hardened remelting layer formed on martensitic stainless steel.

IV. CONCLUSIONS

In martensitic stainless steel, a maximum-level hardening effect can be achieved because of the super-rapid cooling rate caused by laser irradiation. The corrosion resistance of martensitic stainless steel, which is lower than those of other stainless steels, can be significantly improved via laser thermal processing. The cytocompatibility of martensitic stainless steel was effectively modified using the laser thermal processing technique applied in this study.

ACKNOWLEDGMENTS

This research was funded by the Joint Usage/Research Center Program of the Aluminium Research Center (ARC), University of Toyama, and a Grant-in-Aid from the Japan Institute of Metals and Materials (JIMM). This work was also supported by JSPS KAKENHI under Grant No. JP24K01223.

AUTHOR DECLARATIONS

Conflict of Interest

The authors have no conflicts to disclose.

Author Contributions

Y. Tsutsumi: Conceptualization (lead); Formal analysis (equal); Funding acquisition (equal); Methodology (equal); Project administration (equal); Resources (equal); Supervision (lead); Visualization (equal); Writing – original draft (equal); Writing – review & editing (equal). **M. Shimabukuro**: Data curation (equal); Investigation (equal). **T. Manaka**: Data curation (equal); Formal analysis (equal); Investigation (equal); Validation (equal). **M. Goto**: Conceptualization (equal); Funding acquisition (equal); Resources (equal). **M. Kaodowaki**: Data curation (equal); Investigation (equal); Resources (equal); Validation (equal). **T. Hashimoto**: Investigation (equal). **M. Kawashita**: Funding acquisition (equal); Resources (equal); Supervision (equal). **T. Ishimoto**: Funding acquisition (equal); Methodology (equal); Project administration (equal); Supervision (equal). **H. Katayama**: Resources (equal); Supervision (equal).

DATA AVAILABILITY

The data that support the findings of this study are available from the corresponding author upon reasonable request.

REFERENCES

[1] L. D. Barlow and M. Du Toit, J. Mater. Eng. Perform. **21**, 1327 (2012).
[2] C. X. Li and T. Bell, Corros. Sci. **48**, 2036–2049 (2006).
[3] C. X. Li and T. Bell, Mater. Sci. Technol. **23**, 355–361 (2007).
[4] S.-Y. Lu, K.-F. Yao, Y.-B. Chen, M.-H. Wang, N. Chen, and X.-Y. Ge, Corros. Sci. **103**, 95–104 (2016).
[5] Y. Zhao, H. Xiong, X. Li, W. Qi, J. Wang, Y. Hua, T. Zhang, and F. Wang, Corros. Commun. **2**, 55 (2021).
[6] Q. Chao, V. Cruz, S. Thomas, N. Birbilis, P. Collins, A. Taylor, P. D. Hodgson, and D. Fabijanic, Scr. Mater. **141**, 94 (2017).
[7] M. Kazemipour, M. Mohammadi, E. Mfoumou, and A. M. Nasiri, JOM **71**, 3230 (2019).
[8] G. Sander, S. Thomas, V. Cruz, M. Jurg, N. Birbilis, X. Gao, M. Brameld, and C. R. Hutchinson, J. Electrochem. Soc. **164**, C250 (2017).
[9] K. Saeidi, D. L. Zapata, F. Lofaj, L. Kvetkova, J. Olsen, Z. Shen, and F. Akhtar, Addit. Manuf. **29**, 100803 (2019).
[10] Y. Tsutsumi, T. Ishimoto, T. Oishi, T. Manaka, P. Chen, M. Ashida, K. Doi, H. Katayama, T. Hanawa, and T. Nakano, Addit. Manuf. **45**, 102066 (2021).
[11] S. H. Sun, T. Ishimoto, K. Hagihara, Y. Tsutsumi, T. Hanawa, and T. Nakano, Scr. Mater. **159**, 89 (2019).
[12] A. Chiba, I. Muto, Y. Sugawara, and N. Hara, J. Electrochem. Soc. **160**, C511 (2013).
[13] J. E. Castle and R. Ke, Corros. Sci. **30**, 409 (1990).
[14] R. Ke and R. Alkire, J. Electrochem. Soc. **139**, 1573 (1992).
[15] G. S. Frankel, J. Electrochem. Soc. **145**, 2186 (1998).
[16] M. P. Ryan, D. E. Williams, R. J. Chater, B. M. Hutton, and D. S. McPhail, Nature **415**, 770 (2002).
[17] J. H. Park and Y. Kang, Steel Res. Int. **88**, 1700130 (2017).
[18] Y. Tsutsumi, S. Bartakova, P. Prachar, Suyalatu, S. Migita, H. Doi, N. Nomura, and T. Hanawa, J. Electrochem. Soc. **159**, C435 (2012).
[19] Y. Tsutsumi, I. Muto, S. Nakano, J. Tsukada, T. Manaka, P. Chen, M. Ashida, Y. Sugawara, M. Shimojo, N. Hara, H. Katayama, and T. Hanawa, J. Electrochem. Soc. **167**, 141507 (2020).
[20] P. Taxell and P. Huuskonen, Regul. Toxicol. Pharmacol. **133**, 105227 (2022).
[21] P. Naserzadeh, A. Razmi, R. Yesildal, and B. Ashtari, Toxicol. Res. **11**, 286 (2022).
[22] K. T. Oh, Y. S. Kim, Y. S. Park, and K. N. Kim, J. Biomed. Mater. Res., Part B **69B**, 183 (2004).